

DART for adjacent current pattern in Electrical Impedance Tomography

Jae-Hyoung Kim¹, Chan Yong Kim¹, Min Seong Kim¹, Bong-Yeol Choi¹,
Sin Kim², Jeong Seong Lee² and Kyung Youn Kim³

¹Department of Electronic Engineering, Kyungpook National University
Daegu, 702-701, Korea

²Department of Chemical Engineering, Cheju National University
Cheju, 690-756, Korea

³Department of Electrical and Electronic Engineering, Cheju National University
Cheju, 690-756, Korea

E-mail: cjsrkd97@hanmail.net, sinkim@cheju.ac.kr, kyungyk@cheju.ac.kr

Abstract: This work presents the image reconstruction algorithm for EIT that can enhance the speed of image reconstruction and the quality of reconstructed image. The main idea of the proposed algorithm is weighting matrices, which are obtained by the interpolation of the stream lines. Numerical experiments demonstrate that proposed algorithm provides improved reconstruction performance in terms of computational time and image quality.

1. INTRODUCTION

Electrical impedance tomography (EIT) techniques have received a lot of attention from a theoretical and experimental point of view, as they can be used as an imaging modality for monitoring tools in many fields of engineering. They have relatively inexpensive electronic hardware requirements, non-invasive measurement sensing, and a comparatively good temporal resolution [1].

In EIT, the currents are injected through the electrodes mounted on the boundary of the object to be imaged and the excited voltages are measured on the electrodes. It is governed by a partial differential equation (Laplace equation) with appropriate boundary conditions. Based on the current-voltage relationship, the internal resistivity distribution is reconstructed. EIT has received considerable attention in process, chemical, geological, and biomedical engineering areas due to its non-invasive characteristics, low cost requirements, good temporal resolution, and visualization of totally new physiological information. Since, EIT does not use ionizing electromagnetic radiation. Hence, it is safe enough to use as a long term monitor in clinical applications [2].

However, due to the complexity of this relationship, it is usually impossible to obtain a closed-form solution for the resistivity distribution. Hence, numerous reconstruction algorithms have been developed to estimate the internal resistivity distribution of the object. It is well known that conventional EIT imaging techniques, such as the modified Newton-Raphson (mNR) algorithm, and extended Kalman filter (EKF) algorithm, and back projection (BP) algorithm [2, 3, 4, 5].

The mNR and EKF are iterative image reconstruction algorithms. They generally produce improved images however they can only be used off-line because of their intensive computational burden. And the BP algorithm is

non-iterative image reconstruction algorithm. It has a fast calculation time. However, the quality of reconstructed image has a low resolution.

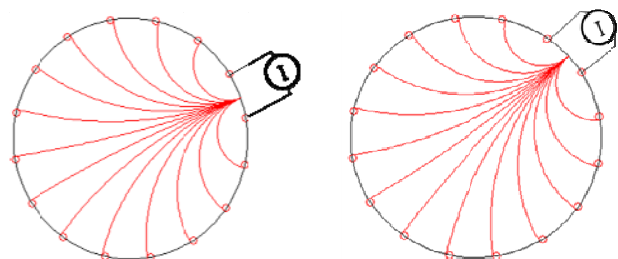
In this paper, we propose directional algebraic reconstruction technique (DART) to enhance the quality of reconstructed image. The weighting matrix used in DART is determined by the interpolation of stream line. It is generated by injected current. Numerical simulation results shown DART give enhanced performance.

2. THE IMAGE RECONSTRUCTION ALGORITHM

There are two types in reconstruction algorithm for EIT. One is linear reconstruction method such as the back-projection, singular value decomposition and etc. Another is nonlinear reconstruction method such as Newton-Raphson method, Extended Kalman filter method and etc. In the point of linear methods, these methods have advantages such as like simple structure and fast calculation time. However, the quality of reconstructed image has low resolution. In this section, we will deal with linear reconstruction method.

2.1 Back-projection

The BP algorithm is used in X-ray Computed tomography (CT). In the CT, it is assumed that all ray-paths are straight line and they path all individual pixels in the domain. In the EIT, These assumptions are impossible. So, the isopotential lines which are formed when adjacent currents are injected through electrodes on the surface were used.



(a) The 1-st current pattern (b) The 2-nd current pattern

Fig. 1. The isopotential lines from adjacent current pattern

Generally, the BP algorithm generally is used to reconstruct an image in EIT [4, 5]. Since, the structure of this algorithm is simple and the calculation time is fast. However, the relationship between the normalized resistivity distribution and normalized boundary voltages is highly nonlinear and ill-posedness. So, the quality of reconstructed image is not satisfactory as reconstruction algorithm.

In BP algorithm, it is assumed that the electrodes are arranged with equidistant spacing around the boundary, the initial resistivity distribution is uniform, and the change in resistivity is small [4, 5].

A simple linear approximation algorithm can be defined as follow:

$$C^* = Sg \quad (1)$$

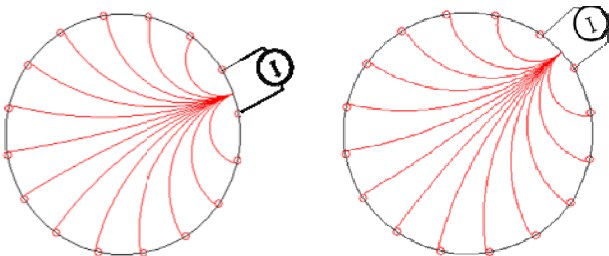
Where, $C^* \in \mathfrak{R}^{N \times 1}$ is the normalized boundary voltage vector, $S \in \mathfrak{R}^{M \times N}$ is the sensitivity matrix and $g \in \mathfrak{R}^{M \times 1}$ is the normalized resistivity vector. M and N are the number of mesh and measured voltages, respectively. An image in the BP is reconstructed by

$$g = S^T C^* \quad (2)$$

2.2 The stream line

The reconstruction algorithms for x-ray CT generally define the ray-path running between the source and detector, which is a straight line with width. However, EIT has 'soft-field' characteristics, it is difficult to find an accurate ray-path. Even if we can find the ray-path, it depends on the parameter distribution inside the domain [6, 7].

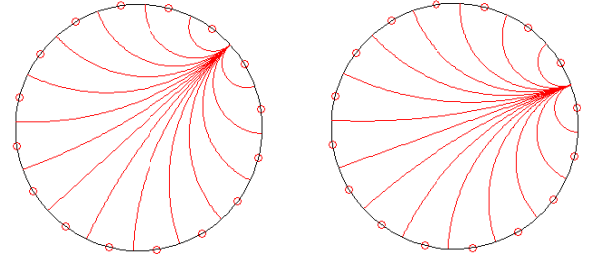
To apply ART in EIT, we use iso-potential lines which are generated when the adjacent current patterns are injected through the attached electrodes on the object. Fig. 2 shows the iso-potential line when 1st and 2nd current patterns are injected for homogeneous. If a L -electrode system is used, the total number of current patterns and iso-potential lines are L and $(L-1) \times L$, respectively.



(a) The 1st current pattern (b) The 2nd current pattern
Fig. 2 The iso-potential lines.

From the iso-potential lines, the stream lines which present the mean value of resistivity distribution between adjacent iso-potential line can be approximated [4, 5, 9].

Fig. 3 shows the stream lines when 1st and 2nd current patterns are injected for homogeneous.



(a) The 1st current pattern (b) The 2nd current pattern
Fig. 3 The stream lines.

To find the resistivity values of stream lines, it is assumed, if the resistivity change is small, the stream lines do not change in case of inhomogeneous. And the resistivity values of stream lines can be defined ratio of the voltage. In this procedure, we do not calculate the resistivity values of the first and last stream lines. Since, we cannot measure voltages at these electrodes. These are denoted as follow:

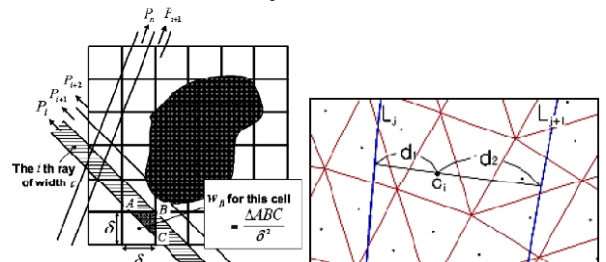
$$\rho_{k,\ell}^{st\,inhomo} = \frac{V_{k,\ell}^{inhomo}}{V_{k,\ell}^{homo}} \times \rho_{k,\ell}^{st\,homo} \quad \begin{cases} k = 2, 3, \dots, L-1 \\ \ell = 1, 2, \dots, L \end{cases} \quad (3)$$

Where, $\rho_{k,\ell}^{st\,inhomo}$ is the resistivity value of k -th steam line and ℓ -th current pattern. $V_{k,\ell}^{inhomo}$ is the voltage difference between adjacent electrodes [4].

2.3 The algebraic reconstruction technique

In x-ray CT, an image is reconstructed using the relationship between ray-path and elements passing by the ray-path (Fig. 4(a)). In most cases in x-ray CT, the ray-path width is approximately equal to the width of image cell and then parallel projections pass through all elements in the domain [7]. But stream lines in EIT do not pass through all elements in the domain (Fig. 4(b)). So, to consider the relationship between stream lines and the elements which are not passed by the stream lines, we define the weighting matrices based on the distance between adjacent stream lines and the elements. Two types of weighting matrices are needed to develop DART [6, 7, 8].

Firstly, the backward matrices W_i^B relate each adjacent stream lines for ℓ -th current pattern to elements which exist between adjacent stream lines. The backward matrix is used to define the resistivity value of elements which are not intersected by the stream lines in domain. We use linear interpolation to define the backward matrix which is based on the distance between adjacent stream lines.



(a) X-ray CT (b) EIT

Fig. 4 The concept of weighting matrix.

The elements which are not passed by steam line in domain can be defined as follow:

$$\rho = W_i^B \cdot \rho^{st_{inhomo}} \quad (4)$$

where , ρ is the internal resistivity vector and $\rho^{st_{inhomo}}$ is the stream line vector for l-th current pattern.

The sensitivity distribution in the domain generally depends on the internal resistivity distribution. However, the closer in the distance between a stream line and an element, the larger in sensitivity factor. Therefore, it is assumed that the existing elements between adjacent stream lines for l-th current pattern only influence the stream lines.

In Fig. 4(b), two lines L_j and L_{j+1} are j-th and j+1-th stream lines for l-th current pattern, respectively and triangles are elements to reconstruct the resistivity distribution in the domain and the point in a triangle is the center of gravity of the triangle. The weighting factors between adjacent the stream lines L_j and L_{j+1} for l-th current pattern and i-th element are defined as:

$$\begin{aligned} W_k^B(i, j) &= \frac{d_2}{d_1 + d_2} & i = 1, 2, \dots, M \\ & & j = 2, \dots, N \\ W_k^B(i, j+1) &= \frac{d_1}{d_1 + d_2} & k = 1, 2, \dots, L \end{aligned} \quad (5)$$

Where , M is total number of element in the domain, N is the number of streams for a current pattern, N is $L-2$. L is the number of electrode. In Eq.(5), 1st and $L-1$ -th stream lines do not use. Because, the currents are injected these electrode.

The forward matrixes W_i^F which relates all elements in the domain to stream lines for l-th current pattern and defined as

$$W_i^F = (W_i^B)^T \quad (6)$$

Using these weighting matrices, DART can be summarized as follows:

$$\begin{aligned} \rho_{\ell+1} &= \rho_{\ell} + W_{\ell}^B (\rho_{\ell}^{st_{inhomo}} - W_{\ell}^F \rho_{\ell}) \\ \ell &= 1, 1 + \frac{L}{4}, 1 + \frac{2L}{4}, 1 + \frac{3L}{4}, \dots, \frac{L}{4}, \frac{2L}{4}, \frac{3L}{4}, L \end{aligned} \quad (7)$$

Where, ρ_{ℓ} is the internal resistivity vector, W_{ℓ}^B, W_{ℓ}^F are the backward and forward weighting matrices for l-th current pattern, respectively. $\rho_{\ell}^{st_{inhomo}}$ is the mean resistivity vector of stream line for l-th current pattern. The iteration in DART is completed after L times update, for L -electrode system. A computation time of DART is significantly fast.

Because, the used FEM mesh for reconstruction and the stream line are fixed a priori. So, weighting matrices can be precalculated off-line. In this reason, on-line computational burden can be reduced significantly in real application.

3. NUMERICAL SIMULATION

To verify the performance of the DART method, we have conducted numerical experiments. We compare the DART with BP algorithm [4, 5]. The BP algorithm is well known by reconstruction algorithm for EIT system. To calculate boundary voltage, we use 3104 mesh as shown in Fig. 5. The FEM meshes in Fig. 5 are the pahntom with 800 mm diameter and 32 electrodes on the surface. For current injection, we use adjacent current patterns. We assume the resistivity values of object and the background are 600Ωcm and 300Ωcm, respectively. We used for three cases to confirm the reconstruction performance of proposed algorithm. Fig. 5 shows the true images used in numerical simulation. The reconstructed images are shown in Fig. 6, 7.

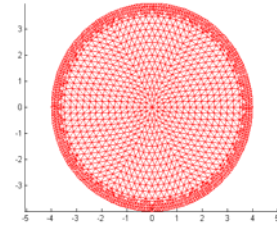


Fig. 5 The FEM Mesh.

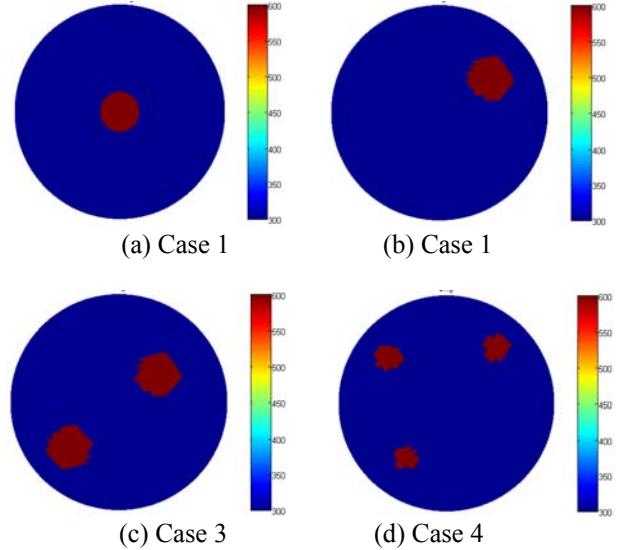


Fig. 6 True resistivity distribution.

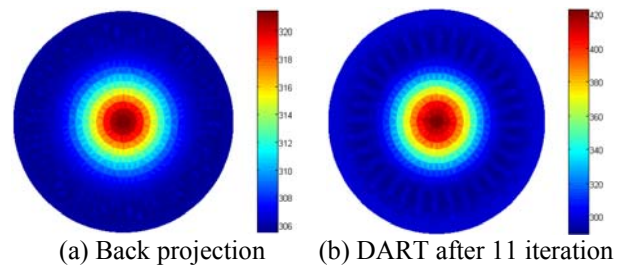


Fig. 7 The reconstructed resistivity distribution for case 1.

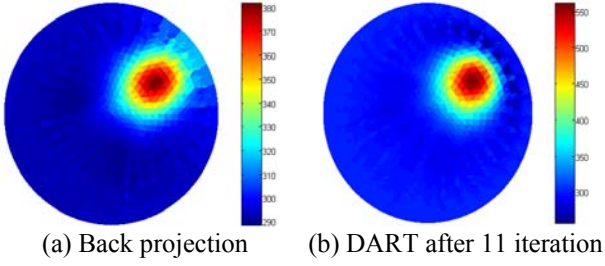


Fig. 8 The reconstructed resistivity distribution for case 2.

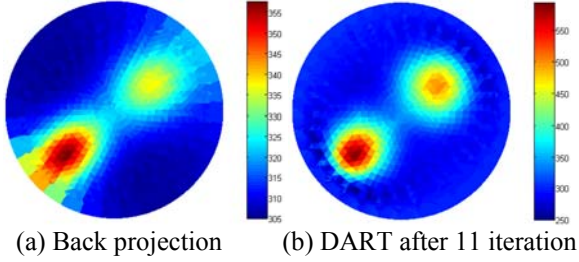


Fig. 9 The reconstructed resistivity distribution for case 3.

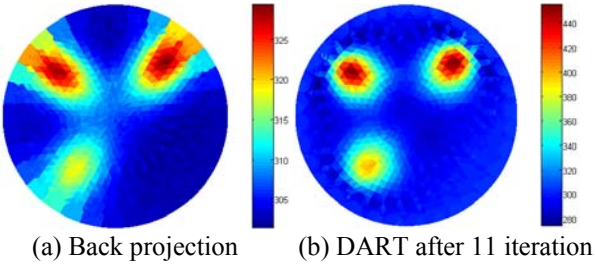


Fig. 10 The reconstructed resistivity distribution for case 4.

From Fig. 7 to 10 are the reconstructed images of BP and proposed algorithm for all cases. The BP and proposed algorithm reveal a good performance for case 1 and 2. However, we can find that the proposed algorithm has the improved image and find more accurate resistivity than BP for case 3 and 4.

In order to evaluate the reconstruction performance more quantitatively, image error (IE) and correlation coefficient (CC) were defined as follows:

$$IE = \frac{\|\hat{\rho} - \rho\|}{\|\rho\|} \quad (8)$$

$$CC = \frac{\sum_{i=1}^M (\hat{\rho}_i - \bar{\hat{\rho}})(\rho_i - \bar{\rho})}{\sqrt{\sum_{i=1}^M (\hat{\rho}_i - \bar{\hat{\rho}})^2 (\rho_i - \bar{\rho})^2}} \quad (9)$$

Where, $\hat{\rho}$ is the resistivity vector of reconstructed image, ρ is the resistivity vector of true image, $\bar{\rho}$ and $\bar{\hat{\rho}}$ are the mean values of ρ and $\hat{\rho}$, respectively. It should be mentioned here, that a smaller IE and CC closer to 1 represent good reconstruction performance. Table 1 shows

the IEs and CCs for all cases. The IEs and CCs of proposed method smaller than that of BP for all cases.

Table 1. IEs and CCs for all cases

	Algorithm	Case 1	Case 2	Case 3	Case 4
IE	BP	0.1510	0.1322	0.1795	0.1390
	DART	0.1177	0.0927	0.1265	0.1145
CC	BP	0.6733	0.5427	0.5236	0.3953
	DART	0.6906	0.7713	0.7597	0.6253

4. CONCLUSION

In this paper, we propose the DART for adjacent current injection pattern in EIT. In the DART, new weighting matrices are obtained based on the interpolation of the between adjacent stream lines. The stream lines are formulated based on the assumption that the resistivity distribution inside the domain is homogeneous. The advantages of the proposed algorithm are weighting matrices can be pre-calculated by off-line since FEM meshes and stream lines are fixed *a priori*. So, the reconstruction time can be reduced significantly. And DART can obtain comparatively good quality image.

References

- [1] J. G. Webster, *Electrical Impedance Tomography*, Bristol, U.K. Adam Hilger, 1990.
- [2] M. Vauhkonen, P. A. "Electrical Impedance Tomography and Prior Information," *Doctoral's thesis, Dept. Applied physics, Univ. Kuopio*, Finland, 1997.
- [3] K. Y. Kim, B. S. Kim, M. C. Kim, Y. J. Lee, and M. Vauhkonen, "Image reconstruction in time-varying electrical impedance tomography based on the extended Kalman filter," *Meas. Sci. Tech.*, vol 18, pp. 62-70, 2001.
- [4] N. J. Avis and D. C. Barber, "Adjacent or Polar Drive?: Image reconstruction implications in Electrical Impedance tomography systems employing filtered back projection," *IEEE*, pp.1689-1690.
- [5] D. C. Barber and B. H. Brown, "Progress in electrical impedance tomography," In: *Inverse Problems in Partial Differential Equations*. Ed D. Colton, R. Ewing and W. Rundel, SIAM, 1990, pp 149-162.
- [6] J. H. Kim, B. Y. Choi, K. Y. Kim, and B. Y. Choi, "Directional Algebraic Reconstruction Technique for Electrical Impedance Tomography".
- [7] J. H. Kim, B. Y. Choi, K. Y. Kim, "Novel Iterative Image Reconstruction Algorithm for Electrical Capacitance Tomography: Directional Algebraic Reconstruction Technique," *IEICE TRANSACTIONS on Fundamentals of Electronics, Communications and Computer Sciences*, E89-A, No. 6 pp. 1578-1584.
- [8] R. Gordon, R. Bender, and G. T. Herman, "Algebraic reconstruction techniques (ART) for three-dimensional electron microscopy and x-ray photography", *J. Theory*.
- [9] Bryan Stroube, Daniel Wilhelm, Justin Woo "Electronic Impedance Tomography"